BREATHING VIBRATIONS OF A CIRCULAR CYLINDRICAL SHELL CONTAINING AN INTERNAL LIQUID

by

H. Norman Abramson
Daniel D. Kana
Ulric S. Lindholm

Technical Report No. 3
Contract No. NASw-146
SwRI Project No. 4-961-2

1 February 1962

[redacted]

SOUTHWEST RESEARCH INSTITUTE
SAN ANTONIO, TEXAS

SOUTHWEST RESEARCH INSTITUTE
8500 Culebra Road, San Antonio 6, Texas

Department of Mechanical Sciences
Engineering Analysis Section

BREATHING VIBRATIONS OF A CIRCULAR CYLINDRICAL SHELL CONTAINING AN INTERNAL LIQUID

by

H. Norman Abramson
Daniel D. Kana
Ulric S. Lindholm

Technical Report No. 3
Contract No. NASw-146
SwRI Project No. 4-961-2

Prepared for

The National Aeronautics and Space Administration
1520 H Street, Northwest
Washington 25, D. C.

1 February 1962

APPROVED:

H. Norman Abramson, Director
Department of Mechanical Sciences

NATIONAL AERONAUTICS AND SPACE ADMINISTRATION

Technical Report No. 3

BREATHING VIBRATIONS OF A CIRCULAR CYLINDRICAL SHELL CONTAINING AN INTERNAL LIQUID

By H. Norman Abramson, Daniel D. Kana
and Ulric S. Lindholm

SUMMARY

Resonant breathing frequencies and mode shapes are determined experimentally for a thin walled, circular cylindrical shell containing a nonviscous incompressible liquid. The resonant frequencies determined for the full shell are in good agreement with those predicted by Reissner's shallow shell vibration theory with the inclusion of an apparent mass term for the liquid. The effect of the internal liquid on the shell mode shapes is significant only for the partially full shell. In this case the circumferential node lines tend to shift toward the bottom or filled portion of the shell.

Excitation of low frequency liquid sloshing motion by the high frequency forced oscillation of a partially filled shell occurred in many cases. This low frequency liquid response is tentatively explained as being excited by a beat frequency in the forced oscillation. A similar type of response has been reported by Yarymovych in axially excited rigid tanks.

INTRODUCTION

The problem of dynamic interaction between liquid motions and elastic deformations of the walls of the container is of fundamental interest and importance with respect to a variety of applications. For example, there is the problem of bending oscillations in long tubes containing static or flowing liquids as encountered in many piping systems, the effect of nonrigid walls on the transmission of acoustic or pressure pulses in liquids or gases in long tubes, and the effect of a free surface on the overall dynamic response of a liquid-tank system. The latter is of particular interest in the design of large liquid propellant rockets, which must be studied as elastic systems rather than rigid bodies because of the stringent requirements for light-weight and strength with the consequent sacrifice in stiffness, and because of the very large percentage of the total vehicle weight contributed by the propellant. The influence of fuel sloshing on rigid body vehicle performance and auto-pilot requirements is given much attention in design and analysis, but thus far little effort has been given to the interaction of the liquid dynamics with the elastic structure.

The work presented in this paper is part of a study pertaining to the dynamic interaction between an internal liquid and the containing elastic tank and is concerned principally with the effect of the internal liquid on the <u>breathing</u> mode shapes and resonant frequencies of a thin circular cylindrical shell[*]. By breathing modes are meant those vibrational modes associated with flexural motion of the shell wall such that the radial displacement is proportional to $\cos n\theta$ where n is an integer greater than or equal to two. $n=0$ and $n=1$ correspond to rotationally symmetric and beam bending vibrations, respectively. Any mode shape can then be specified by two parameters, m and n both integers. If the radial displacement of the wall can be taken as proportional to $\sin \frac{m\pi x}{L}$ in the axial direction, $m+1$ defines the number of node lines encircling the cylinder, including those at each end, and $2n$ defines the number of node lines parallel to the axis of the cylinder. Any combination of m and n therefore defines a unique mode and an associated resonant frequency. A large number of resonances are thus possible, even within a limited frequency range.

Previous investigators have reported on the experimental determination of empty and pressurized shell vibration behavior. Each of these has noted the large number of resonances present and the need for careful identification of each resonance with the proper mode shape. This becomes increasingly difficult because the order of the resonant frequencies does not follow from the relative complexity of the mode shape, i.e., a mode with a

---

[*] The results of work relating to the interaction between the internal liquid and the <u>bending</u> vibrations of the elastic tank will be reported in a separate paper.

large number of circumferential nodes may have a lower resonant frequency than one with fewer circumferential nodes. For this reason, for a cylindrical shell, there may occur several resonant breathing frequencies lower than the fundamental bending frequency. Perhaps the first to demonstrate clearly the complex nature of the shell vibration problem were Arnold and Warburton (1, 2)* who performed a comprehensive analytical and experimental study, taking into account a wide range in dimensions and end conditions. These authors showed theoretically that the order in which the resonances occur is determined by the proportion of strain energy contributed respectively by bending and stretching of the shell wall. Their experimental frequency determinations were made by exciting steel cylinders at one point with an alternating magnetic field produced by an oscillator driven electromagnet. Mode shapes were determined by rotating the shell and locating the nodes by means of the sound intensity with a stationary stethoscope. This method of mode determination is somewhat unsure in that one relies on the slight imperfections in the shell to fix the nodal lines. For a perfectly symmetric shell the location of the nodal lines are indeterminate.

Succeeding investigations have extended the studies of cylindrical

---

* Numbers in parentheses refer to the List of References at the end of the paper.

shell vibration to include internal pressurization and improved measurement techniques. Fung, Sechler, and Kaplan (3) studied pressurization effects using a loudspeaker as the excitation source and a number of capacitance probes mounted internal to the cylinder to record wall displacements. Their results showed that the resonant frequencies and, particularly, the order in which the lowest resonant frequencies occur depends significantly upon the internal pressure. Gottenberg (4) extended the experimental techniques to include not only the identification of each mode but the actual measurement of mode shapes. Radial wall displacement was measured with a sensitive condenser microphone mounted on tracks so that it could traverse the specimen in both the axial and circumferential direction thus enabling a complete mapping of the deflection surface. A similar technique is used in the present study in order to determine the effect of the internal liquid, not only on the resonant frequencies of the shell, but also to show any change in a given mode shape caused by the presence of the liquid.

CALCULATION OF SHELL FREQUENCIES

If we assume the radial displacement of the thin walled, circular cylindrical shell containing an internal liquid as

$$w(x,\theta,t) = A_{mn} \sin \frac{m\pi x}{L} \cos n\theta \cos \omega t \qquad [1]$$

the simplified frequency equation of Berry and Reissner (5) is applicable. For the unpressurized shell, this frequency equation can be written as

$$(m_s + m_L) 4\pi^2 f_{mn} = \frac{D}{a^4}\left(\lambda_m^2 + n^2\right)^2 + \frac{Eh}{a^2}\frac{\lambda_m^4}{(\lambda_m^2 + n^2)^2} \qquad [2]$$

where the bending stiffness coefficient $D = \frac{Eh^3}{12(1-\nu^2)}$, the axial wave number $\lambda_m = \frac{m\pi a}{L}$, E = Young's modulus, ν = Poisson's ratio, h = wall thickness, a = radius, and L = total length of the shell. m_s is the mass per unit area of the shell and m_L is an apparent mass of the contained liquid. This frequency equation is based on the approximate shallow shell equations of Reissner which have been shown to give satisfactory results for the empty shell (3,4). The "shallow shell" condition implies that each shell segment between axial node lines acts essentially as a slightly curved plate. Obviously, as n increases, this condition is more nearly satisfied. The boundary conditions at $x=0$ and $x=L$ restrict the radial motion to zero but place no restraint on the axial or tangential displacement.

An expression for the apparent mass, m_L, of the liquid can be obtained by considering the unsteady pressure exerted by the liquid on the shell wall. The effect of the static pressure distribution on the shell wall due to the liquid column is neglected. For small motion of an incompressible liquid, the unsteady pressure, $q(t)$, must satisfy the equation

$$\frac{\partial^2 q}{\partial r^2} + \frac{1}{r}\frac{\partial q}{\partial r} + \frac{1}{r^2}\frac{\partial^2 q}{\partial \theta^2} + \frac{\partial^2 q}{\partial x^2} = 0 \ .$$

The solution of this equation, corresponding to the boundary conditions imposed by the assumed tank motion, is

$$q = C_{mn}\, I_n\left(\frac{m\pi r}{L}\right) \sin\left(\frac{m\pi x}{L}\right) \cos n\theta \, \cos \omega t$$

where the I_n are modified Bessel functions of the first kind of order n. If v_r is the radial component of velocity in the liquid and ρ_L the mass density of the liquid,

$$\frac{\partial v_r}{\partial t} = -\frac{1}{\rho_L}\frac{\partial q}{\partial r}$$

Substituting for q,

$$\frac{\partial v_r}{\partial t} = -\frac{1}{\rho_L}\left(\frac{m\pi}{L}\right) C_{mn}\, I_n'\left(\frac{m\pi r}{L}\right) \sin\left(\frac{m\pi x}{L}\right) \cos n\theta \cos \omega t$$

$$= -\frac{1}{\rho_L}\left(\frac{m\pi}{L}\right) \frac{I_n'\left(\frac{m\pi r}{L}\right)}{I_n\left(\frac{m\pi r}{L}\right)} \cdot q$$

Imposing the continuity boundary condition at the interface between the liquid and the shell,

$$\left.\frac{\partial v_r}{\partial t}\right|_{r=a} = \frac{\partial^2 w}{\partial t^2}$$

and

$$\left. q \right|_{r=a} = -a\rho_L \frac{I_n(\lambda_m)}{\lambda_m I_n'(\lambda_m)} \frac{\partial^2 w}{\partial t^2} \quad .$$

The unsteady pressure exerted by the liquid on the shell is thus proportional to an acceleration term, the coefficient of which is the apparent mass, m_L , in the frequency equation. Thus,

$$m_L = a\rho_L \frac{I_n(\lambda_m)}{\lambda_m I_n'(\lambda_m)} \quad . \qquad [3]$$

The frequency equation [2] can now be rewritten in nondimensional form as

$$4\pi^2 a^2 \frac{\rho_s}{E} f_{mn}^2 = \left[1 + \frac{a}{h}\frac{\rho_L}{\rho_s}\frac{I_n(\lambda_m)}{\lambda_m I_n'(\lambda_m)}\right]^{-1}\left[\frac{(h/a)^2}{12(1-\nu^2)}\left(\lambda_m^2+n^2\right)^2 + \frac{\lambda_m^4}{(\lambda_m^2+n^2)^2}\right] \qquad [4]$$

As either m or n increase, i.e., as the effective wave lengths decrease, the contribution of the apparent liquid mass to the total vibrating mass decreases. Thus, the resonant frequencies of the higher order modes are decreasingly affected by the presence of the liquid.

APPARATUS

The excitation, detection, and recording systems were designed to permit accurate measurement of the resonant frequencies and wall displacement. Excitation of the thin steel shells was provided by an electromagnet driven by an oscillator. A movable, non-contacting displacement probe was used to map the deflection surface, similar to the method of Gottenberg (4).

The shell used in these experiments was manufactured from 4130 steel tubing. After honing out the inside diameter, the tube was placed on a solid mandrel and the outside diameter was ground to a wall thickness of 0.0099 inch. Even with the care taken, deviations from the average wall thickness of ± 0.0010 inch were present. The mean radius of the shell was 1.485 inch and the effective length was 9.00 inches. The ovality was held to within one wall thickness.

The shell was supported vertically in the test fixture shown in Figure 1. The test fixture will accommodate shells of varying lengths, by means of the adjustable top crosshead, and varying end supports which mount on the bottom plate and crosshead. For breathing vibrations, the end fixtures supplied essentially line support so that the ends were maintained circular but were not restrained from axial displacement or rotation. For the liquid filled shell, the bottom end was sealed with a gasket compound.

Because of the thinness of the shell wall and the low mass of the entire shell, it was necessary to use an excitation and detection system that did not contact or add additional mass to the shell and thereby alter the resonant frequencies or mode shapes. Excitation was supplied by an electromagnet driven by an audio oscillator through a 200 watt power amplifier The point of excitation could be moved axially in order to optimize the excitation of different axial modes. The displacement probe was a Bently D-152 Distance Detector, which is an electro-mechanical transducer measuring displacement between the sensing head and the conductive surface of the shell. The probe is non-contacting, has an essentially linear output over a restricted range in displacement, and has ample frequency response for the present application. Static calibration curves for the probe are given in Figure 2. The sensitivity, and to some extent the linearity, of the probe may be changed by varying the voltage drive to the sensing head. Thus, several curves are given in Figure 2 corresponding to different excitation voltages. For the mode shape measurements, the static distance of the probe head from the shell was held constant so that the small dynamic displacements were limited to a linear range of the probe. This was done by monitoring the d-c output of the probe. For ease in properly identifying each mode, two probes were employed; one was a stationary probe located near the top of the shell (see Figure 1), and the second, a movable probe mounted on a circular slide ring concentric with the shell. The ring to which the second probe was attached slides within an axial position ring, allowing the probe to traverse the complete circumference of the shell. An axial traverse of the tank was obtained by turning a lead screw threaded through the axial position ring so that the probe could be raised or lowered over the entire length of the tank. Horizontal alignment of the axial position ring was maintained by the support at the screw and two separate ball bushing supports. The output from the stationary and movable probe was viewed as an X-Y presentation on an oscilloscope so that phase changes could be determined. The number of phase changes in one axial and one circumferential traverse identified a particular mode.

With proper amplification of the output from the displacement probes, wall displacements as small as 10 microinches could be resolved (at the higher frequencies this sensitivity was needed). The frequency at resonance was accurately determined with an electronic, crystal controlled, frequency counter, connected to the output of one of the probes. A general view of the instrumentation is seen in Figure 3.

EXPERIMENTAL RESULTS

Resonant Frequencies of the Empty and Full Shell

Figures 4 and 5 are frequency plots of a large number of modes for the empty shell and the same shell completely filled with water. The experimental frequencies are compared with those obtained from the frequency equation (Eq. [4]). In representing the data, the nondimensionalized frequency parameter $2\pi a\sqrt{\frac{\rho_s}{E}}\, f_{mn}$, is plotted against the axial wave number $\lambda_m = \frac{m\pi a}{L}$, for varying values of n. In this form, the curves represent continuous functions that may be applied to tanks of arbitrary length having the same cross sectional ratio $\frac{h}{a}$, Poisson's ratio ν, and density ratio $\frac{\rho_s}{\rho_L}$. For the tank employed here, the nondimensional frequency corresponds to a frequency range of 0 to 10,000 cps for the empty shell, and 0 to 6,000 cps for the full shell.

The agreement between theory and experiment is seen to be relatively good. The differences that do occur seem to be reflected similarly in both the empty and full shell, indicating that any errors are introduced by the shell equations rather than by the apparent mass loading of the liquid. Before discussing possible sources of error, we might first comment upon the experimental accuracy of the frequency determinations. The actual recording of the frequencies was done with a crystal controlled counter so that this accuracy is within $\pm$ 1 cps. There is the possibility of some error in locating the resonant frequencies by determining the peak amplitude response viewed on the oscilloscope screen. The accuracy here is, of course, dependent upon the sharpness of the resonance but in almost all cases is within ± 5 cps. The exceptions to this occurred in a few cases when a double resonance peak existed for the same mode. These double peaks have been explained by Tobias (6) to be the result of initial imperfections or deviations from rotational symmetry of the circular cylinder, such as variations in the radius, wall thickness, or physical properties of the shell. These imperfections in the shell, which are always present even when particular care is taken in manufacture, produce two preferential planes of vibration for each mode. Excitation in each of the preferential directions produces an amplitude maximum at a slightly different resonant frequency. If the excitation is in other than one of the preferential directions, a double resonance peak may occur. The frequency separation of the two peaks is to some extent a measure of the degree of imperfection. Frequency errors due to this source could be as high as 12 cps. Another observed effect, which may be partly due to shell imperfections and partly to coupling between two closely spaced resonances, is that the nodes are not always positions of zero radial displacement but rather relative minimums in displacement. Thus, phase measurement is the most reliable method for mode determination. The overall accuracy in measuring frequency is within one percent.

The difference between theory and experiment in the frequency plots is seen to increase with increasing n, approaching 4% at $n = 14$. For low values of n the experimental points are lower than the theoretical, which is to be expected owing to the shallow shell approximations in the theory. A comparison of the Reissner shell theory with a more exact theory is given in (3), which shows that after $n = 4$ or 5 the shallow shell approximation becomes accurate. The increase in the experimental frequencies over the theoretical at large values of n is probably due to deviation from the measured average value of the wall thickness or radius of the shell. As n increases, the resonant frequencies become increasingly sensitive to h/a, since the bending term in the frequency equation predominates at these higher modes. A 4% change in the wall thickness, which is within the tolerance of the extremely thin walled shell used, would compensate for the observed deviations from theory. Other sources of error may occur in the values used for the physical properties of the steel, end conditions, or rotary inertia and shear corrections. Undoubtedly, there was some deviation from the theoretical "free" end condition which would tend to raise the shell frequencies. However, this end restraint should have more effect on the modes with fewer axial waves (lower m), which does not appear to be the case. Also, the mode shape measurements do not indicate any appreciable restraint to rotation at the ends.

Corrections for rotary inertia and shear by using a refined theory would decrease the theoretical values, creating an even greater discrepancy. In this respect, these experiments attest to the practicality of using an approximate theory. Although the apparatus, we feel, is sufficient to measure frequency shifts of the order that might be predicted by a refined theory, errors due to reasonable tolerances on the shell dimensions may more than compensate for any improved accuracy in the theory.

Mode Shapes for Full and Partially Full Shells

Measurements of a large number of mode shapes for the empty, full and partially full shell were made in order to determine the effects of the contained liquid. The data is given in terms of the fractional depth b/L, where b is the distance from the bottom of the shell of length L to the surface of the liquid. For comparative purposes, the mode shape plots are normalized by the maximum deflection. The actual magnitudes of the deflections were on the order of 0.0002 inch.

Figure 6 shows a plot of circumferential modes $n=3$, and $n=4$ for the empty shell. The presence of the liquid does not affect the symmetry of the circumferential wave form, as is expected, but does diminish the amplitude response.

Figures 7 through 10 show the axial wave forms for $n=5$ and $m=1, 2, 3, 4$ for the empty, 1/4, 1/2, 3/4, and completely full shell. Comparing the empty and full shell, the static pressure gradient in the liquid filled shell does not appear to have any significant effect upon mode shape. For $m=1$ and $m=2$, the empty and full shell mode shapes are essentially the same. For the higher order modes ($m=3$ and $m=4$) there exists some divergence, principally in the relative amplitudes. This divergence is not felt to be significant because of the difficulty in obtaining a clean mode shape at the higher frequencies. As can be seen from the frequency plots, the resonances become very closely spaced, making it difficult to isolate a single resonance. Many of the mode shapes measured at the higher frequencies showed severe distortion due to coupling with a neighboring resonance, again indicating the necessity for phase determination in properly identifying modes.

For the partially filled tank, the liquid level is seen to have a marked effect upon the mode shape. In general, the position of the axial nodes and antinodes are shifted toward the bottom or filled portion of the shell, the shift being greater the lower the liquid level. However, when the level is very low, as in the 1/4 full case, the nodes in the upper or unfilled portion of the shell tend to return to their normal position. This is especially noticeable for the $m=3$ and $m=4$ modes. Also, the amplitude response of that portion of the tank in contact with the liquid is appreciably decreased.

Effect of Fluid Depth on Resonant Frequencies

The frequency transition from the empty shell to the full shell is indicated for a number of breathing modes by the curves in Figure 11. Frequency measurements were taken at 1/4 depth intervals. These curves clearly show that the order in which the resonances occur depend upon the fluid level. For instance, for the empty shell $f_{1,2}$ is greater than $f_{1,5}$, while this order is reversed for the full shell, with the cross-over occurring slightly above the half full level. At the cross-over point, the two modes have the same resonant frequency.

It is also interesting to note that the shape of the curves seems to depend upon the number of axial waves. The curves with $m=1$, given by the solid lines, all have the same form with the maximum slope or change in frequency occurring at a fractional depth of about 1/4. For $m=2$, given by the dashed lines, there appears to be a decreasing sensitivity to change in liquid level near the 1/2 full shell with increasing sensitivity near the 1/4 and 3/4 depth levels. This is possibly associated with the location of the axial nodes and antinodes.

Free Surface Motion of the Liquid

Although the previous discussion has been concerned principally with the shell response, the dynamic behavior of liquids in partially filled tanks is also of interest and has been given considerable attention in recent years as a result of problems associated with fuel sloshing in missile propellant tanks (7). The fundamental liquid resonances generally occur at low frequencies, governed by the geometry of the container, as compared with the higher resonant frequencies associated with the elastic behavior of the container itself. Thus, it would not be expected that large amplitude liquid free surface motion could be excited by the high frequency breathing vibrations of the tank. This, however, did occur in many cases. In almost all of our experiments, when the partially filled shell was excited at or near one of the resonant elastic breathing frequencies, it was possible to obtain large amplitude, vertical free surface motion of a low frequency. Thus, a sustained low frequency liquid sloshing motion was excited by the high frequency forced vibration of the elastic container.

A similar type of phenomena has been reported by Yarymovych (8) who observed low frequency sloshing motion in a "rigid" tank excited axially at frequencies from 80 to 150 cps. In this case, the axial oscillation of the entire tank produced a dense spray on the surface of the liquid as a result of the break-up of small capillary waves. Yarymovych offered the hypothesis that the low frequency surface resonance was sustained by a proper phasing of the majority of the droplets being released from and impacting on the surface. In the present elastic tank experiments, the high frequency excitation produced very short wave length, low amplitude, surface waves or ripples. These waves emanated from the circumferential antinodes of the shell wall so that the tank motion was readily apparent from observation of the liquid surface. As the forcing amplitude was increased, spray began to form at the antinodes and the low frequency sloshing started. The low frequency liquid surface mode was rotationally symmetric, the first mode having a sharp peak in the center, with higher modes also having been observed. The first two modes are shown schematically in Figure 12a. In some cases, the peak amplitude for the first mode was as large as one inch, the motion being extremely violent.

Because of the amplitude of excitation, the formation of spray generally accompanied the low frequency phenomena. The spray formation, however, did not appear to be the significant factor in supporting the low frequency sloshing (suppression of the spray did not affect the motion). An alternative explanation, suggested by the motion of the shell wall, can also be offered. Figure 12b shows an oscilloscope record of the wall displacement during the low frequency liquid resonance. The same response at two sweep speeds is shown. The records were obtained for a 1/2 full shell excited in the mode $m=1$, $n=4$. The high frequency signal is 375 cps, corresponding to the coupled shell-liquid resonance for that mode, while the low frequency envelope is approximately 5 cps. The shape of the low frequency envelope is similar to that of a beat frequency in forced vibration, which offers a possible explanation for what is happening in this case. With the free surface occurring at an axial antinode of the shell vibration and the forcing frequency in the neighborhood of the free vibration resonance, a beat frequency equal to the difference between the forcing and resonant frequency is established. Under normal conditions, beating occurs between the forced and free vibrations, but because the latter are rapidly damped out, the phenomenon is a transient one; however, in the present case, the beat frequency occurs at a second resonance of the system, the free surface resonance.

Apparently, this coincidence of the free surface resonance with the beat frequency is the mechanism which sustains the motion. The theoretical resonant frequency corresponding to the first rotationally symmetric liquid mode as shown in Figure 12a is 5.03 cps, which agrees well with the observed beat frequency in the tank response.

The similarity in the results of the present experiments and those of Yarymovych raise the question of whether the high order subharmonic liquid response in each case is the result of the same mechanism. The presence of the observed second and third low frequency liquid modes and the non-effectiveness of suppressing the spray make it difficult to explain the present results with the Yarymovych spray hypothesis. Rather, the essential factor appears to be the presence of the elastic resonances of the liquid container itself. It will be necessary to obtain more accurate measurements of the liquid surface mode shapes and phase relationships before this curious phenomenon can be completely explained. Until that time, the practical significance of this phenomenon in rocket propellant tanks will remain unknown.

CONCLUSIONS

The use of the Reissner shallow shell frequency equation with the inclusion of an apparent mass term appears adequate to predict the resonant frequencies of a circular cylindrical shell containing an internal liquid column. The large number shell resonances possible and the irregular order in which these resonances occur make a complete mapping of the shell deflections and phase relationships necessary in order to associate each resonance with the correct mode.

The effect of the internal liquid on the shell mode shape was only evident in the partially filled shell, in which case the mode shape may be severely distorted with the circumferential node lines shifting toward the filled portion of the shell. Experimental results for the effect of fluid level on the resonant frequency of a given mode, indicate that the change in frequency with fluid level is dependent upon the number of axial waves.

The occurrance of sustained large amplitude, low frequency liquid free surface motion in partially filled shells excited by high frequency forced vibration of the elastic container was observed. This phenomena is tentatively attributed to a beat frequency in the forced shell vibration exciting the liquid. This seemingly curious behavior would be worthy of further research in order to determine its practical significance in missile propellant tanks.

ACKNOWLEDGEMENTS

The authors wish to express their appreciation to the SwRI Computations Laboratory for performing the theoretical calculations, to Mr. Gilbert Rivera for preparing the figures, and to Mr. W. H. Chu for valuable discussions.

REFERENCES

1. Arnold, R. N. and Warburton, G. B., "Flexural Vibrations of the Walls of Thin Cylindrical Shells Having Freely Supported Ends," Proc. of the Roy. Soc. (London), A197, p. 238, (1949).

2. Arnold, R. N. and Warburton, G. B., "The Flexural Vibrations of Thin Cylinders," J. Proc. Inst. Mech. Eng. (London), 167, pp. 62-74, (1953).

3. Fung, Y. C., Sechler, E. E., and Kaplan, A., "On the Vibration of Thin Cylindrical Shells Under Internal Pressure," J. Aeronautical Sci., 27, pp. 650-661, (1957).

4. Gottenberg, W. G., "Experimental Study of the Vibrations of a Circular Cylindrical Shell," J. Acoustical Soc. Am., 32, pp. 1002-1006, (1960).

5. Berry, J. G. and Reissner, E., "The Effect of an Internal Compressible Fluid Column on the Breathing Vibrations of a Thin Pressurized Cylindrical Shell," J. Aeronautical Sci., 25, pp. 288-294, (1958).

6. Tobias, S. A., "A Theory of Imperfection for the Vibration of Elastic Bodies of Revolution," Engineering, 172, pp. 409-411, (1951).

7. Abramson, H. N. "Liquid Dynamic Behavior in Rocket Propellant Tanks," ONR/AIA Symposium on Structural Dynamics of High Speed Flight, Los Angeles, April 24-26, pp. 287-318, (1961).

8. Yarymovych, M. I., "Forced Large Amplitude Surface Waves," D. Sc. Thesis, Columbia University, December 1959.

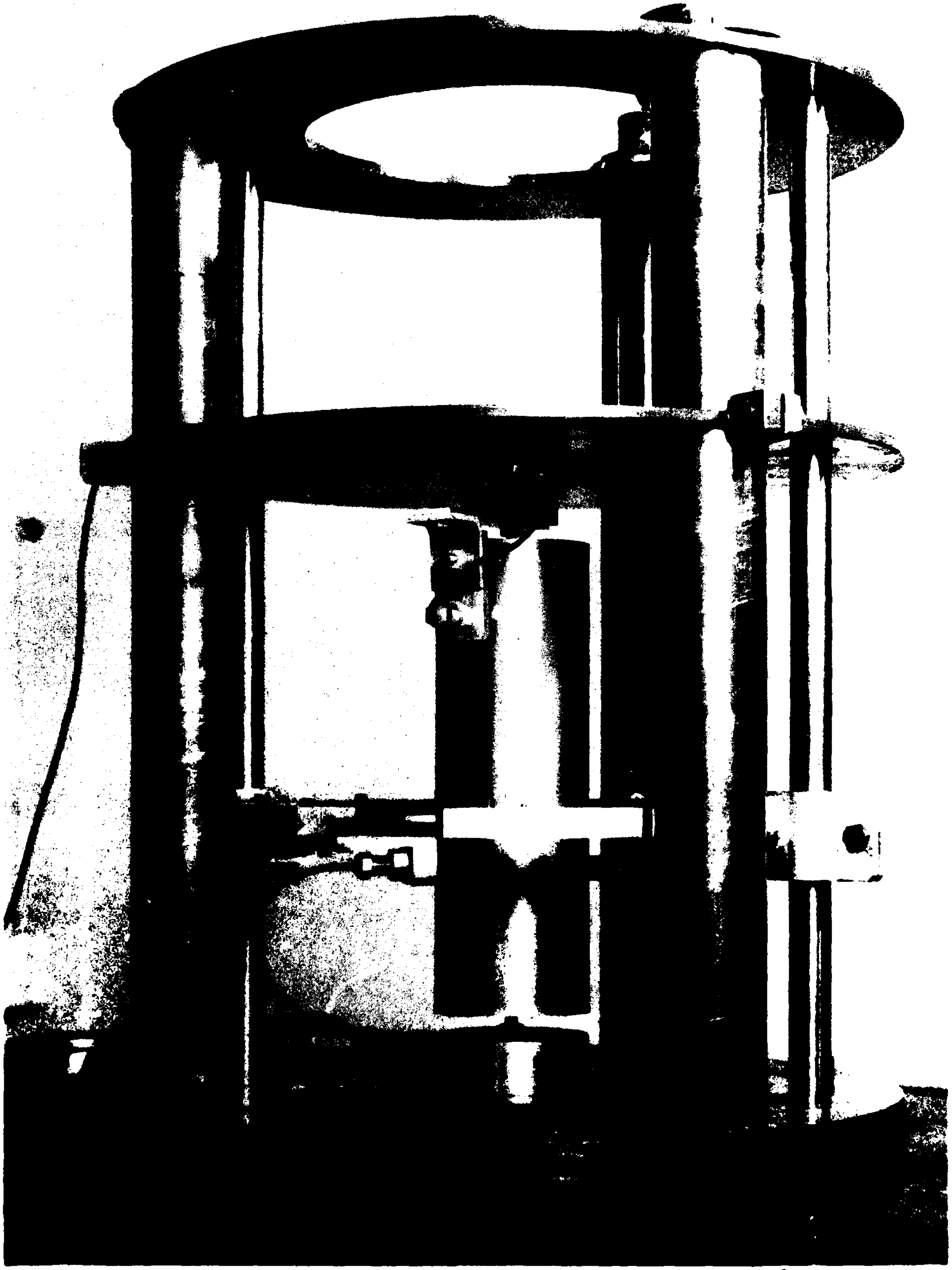

FIGURE 1   Cylindrical Shell Test Fixture

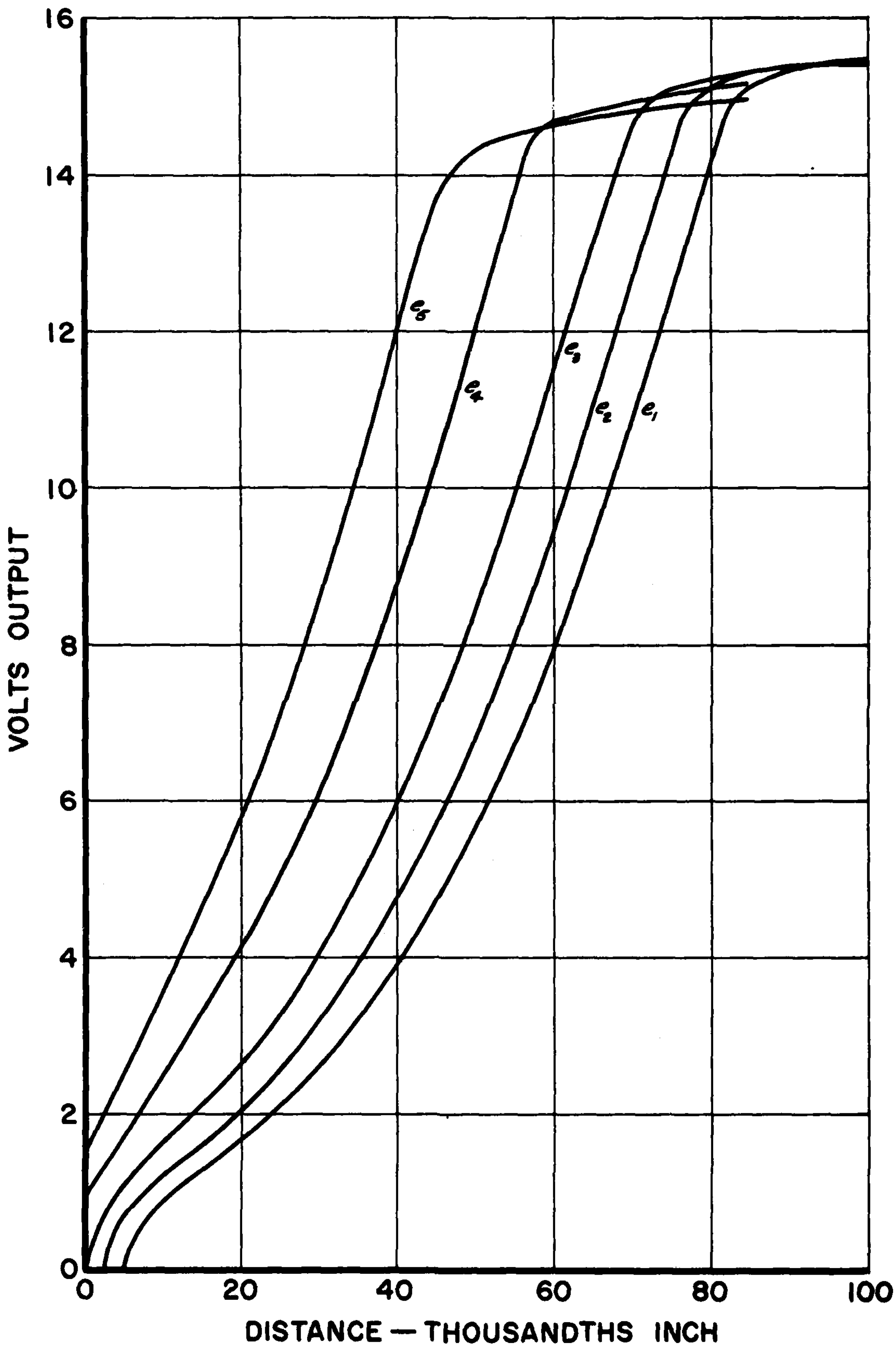

FIGURE 2 Displacement Probe Calibration Curves for Varying Excitation Voltages

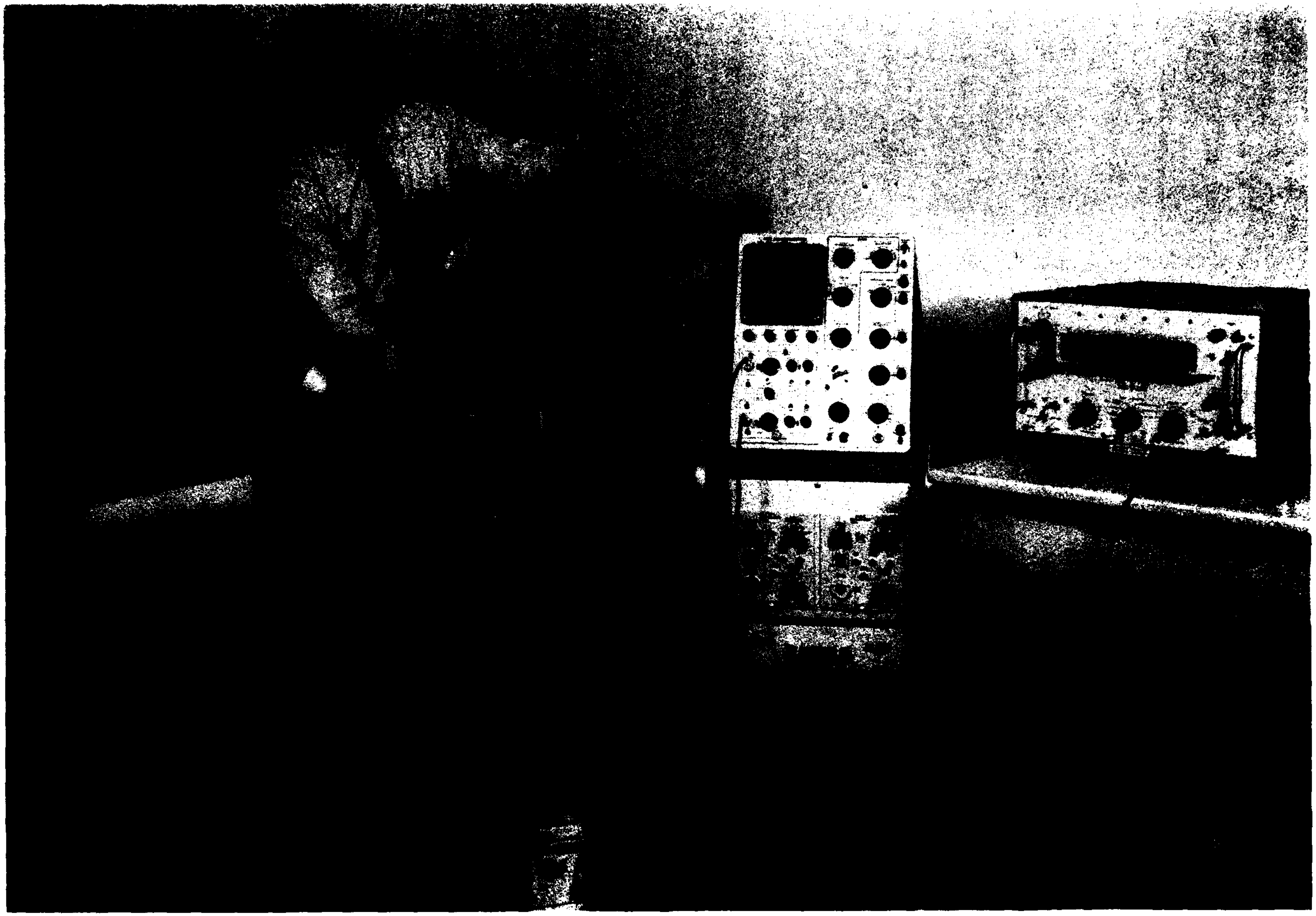

FIGURE 3 General View of Apparatus and Instrumentation

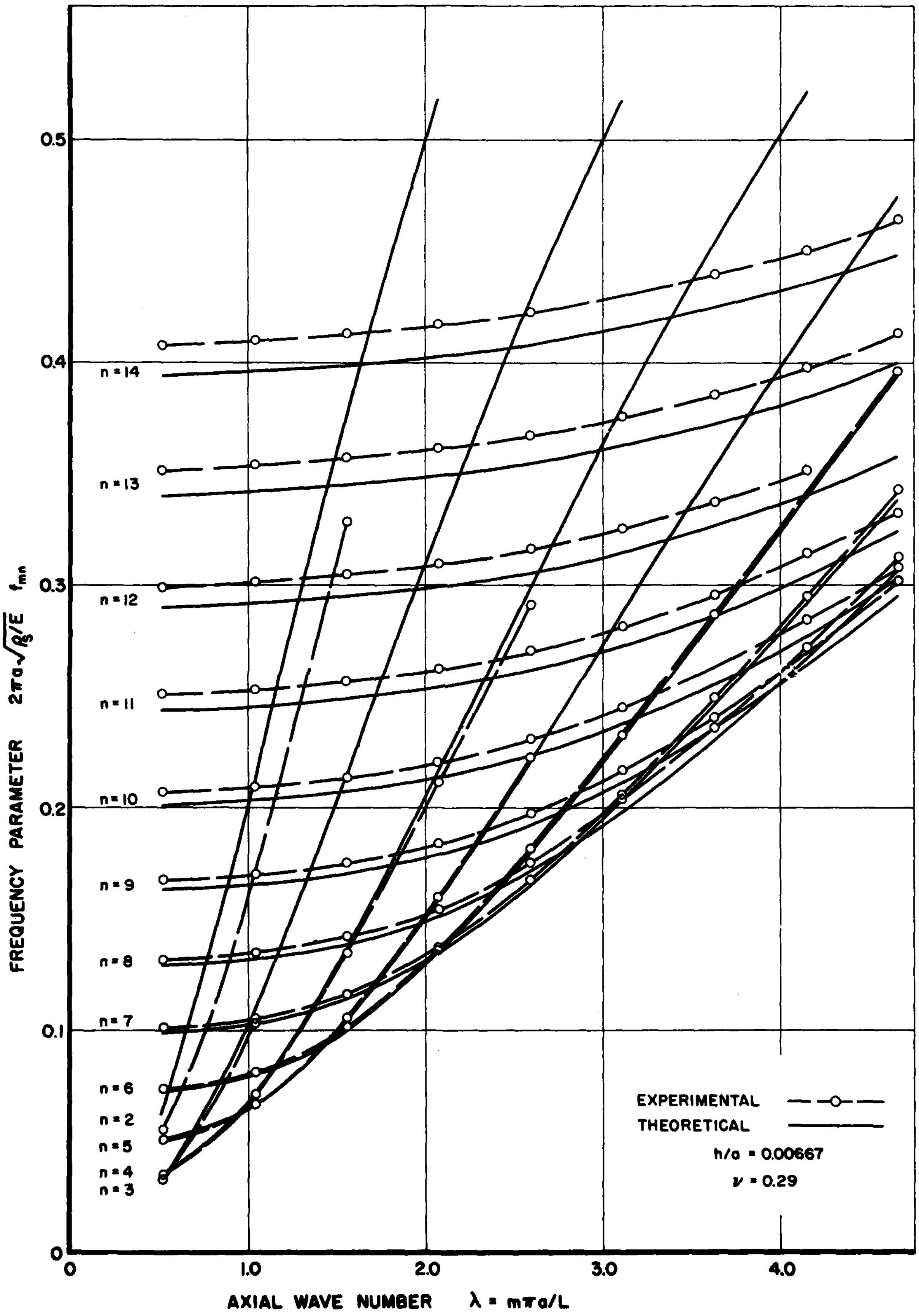

FIGURE 4 Comparison of Experimental and Theoretical Resonant Breathing Frequencies for the Empty Shell

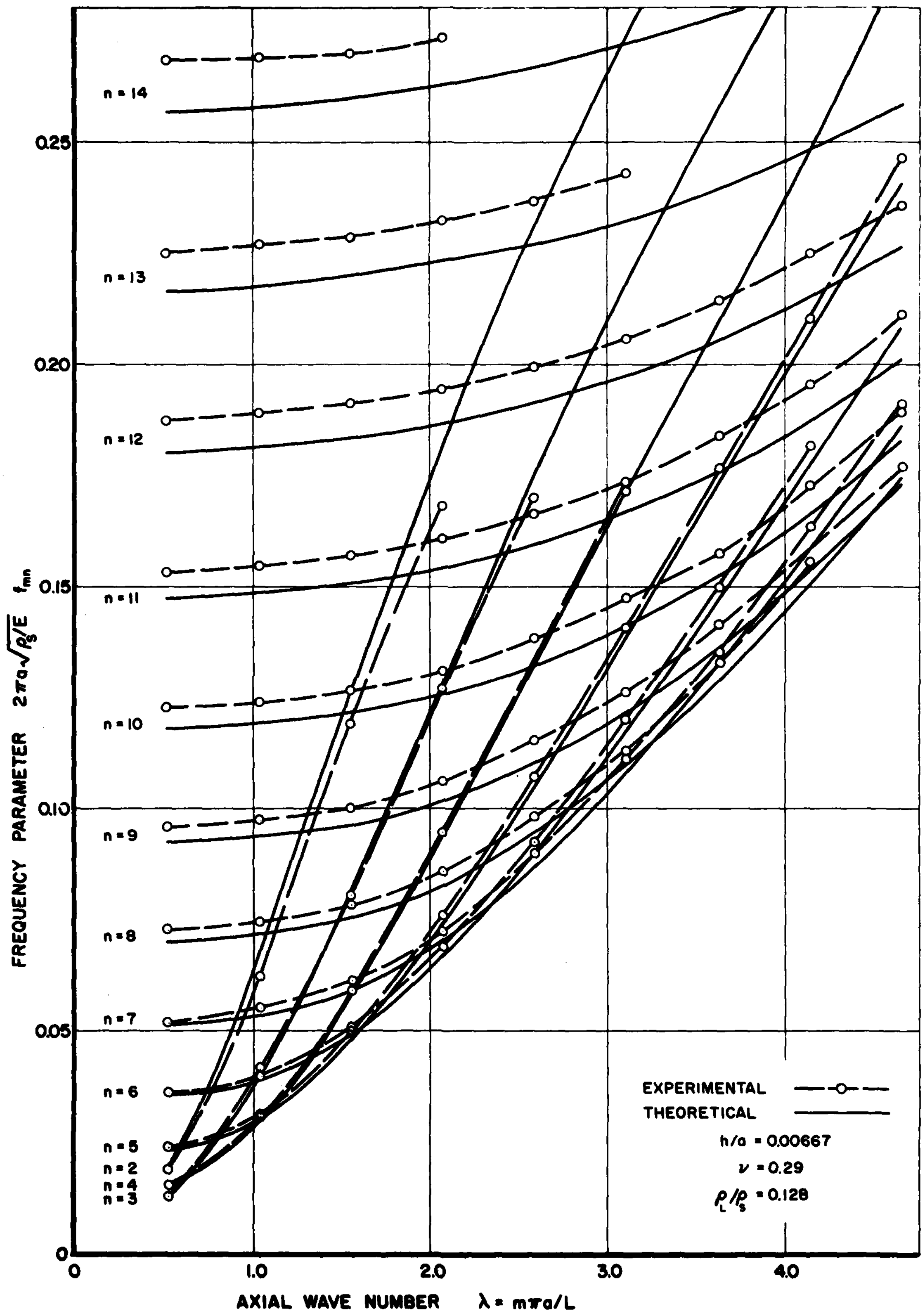

FIGURE 5 Comparison of Experimental and Theoretical Resonant Breathing Frequencies for the Full Shell

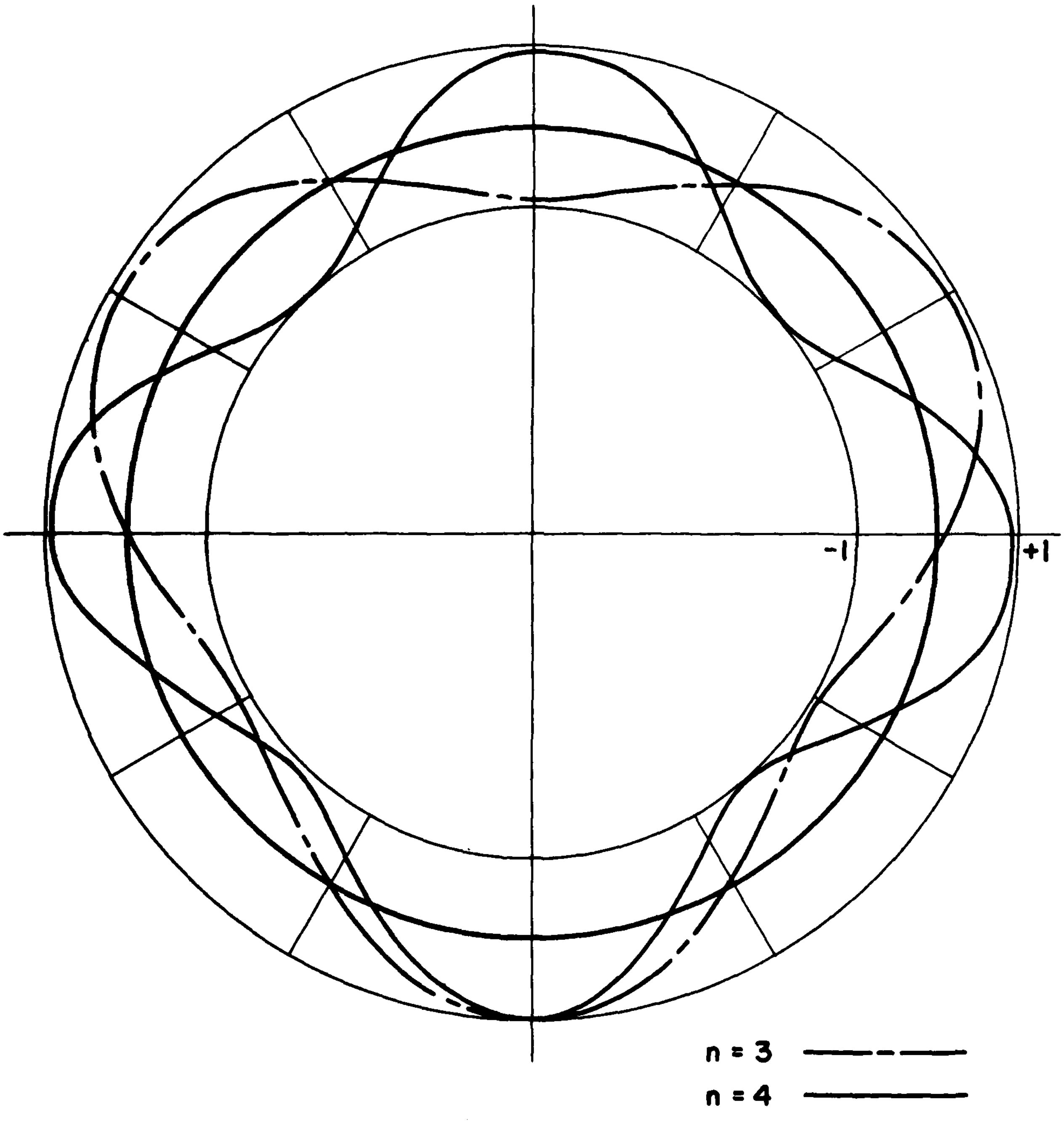

FIGURE 6 Circumferential Mode Shapes for n = 3 and n = 4

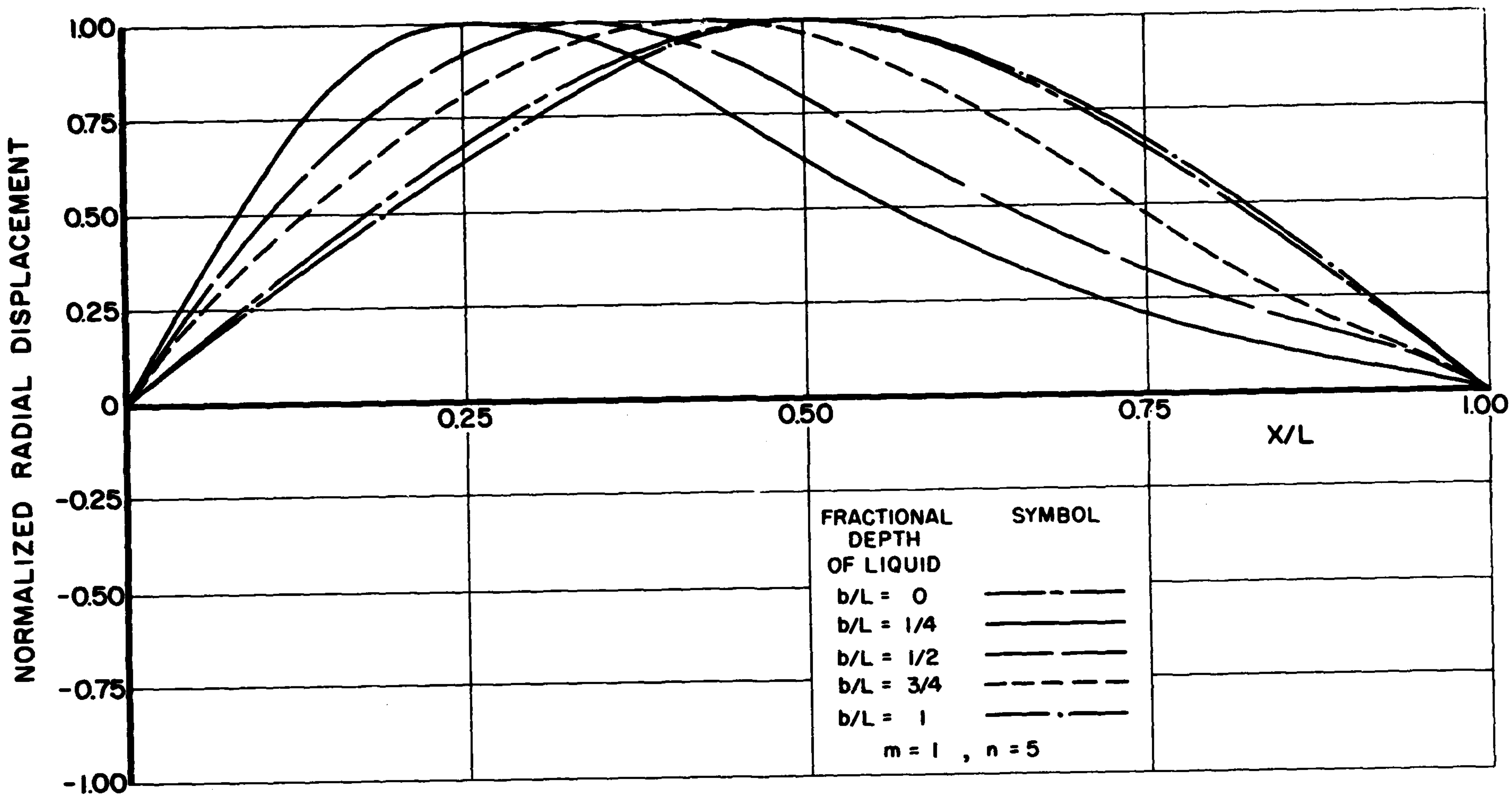

FIGURE 7 Axial mode shapes, $m = 1$, $n = 5$, at Varying Liquid Depths

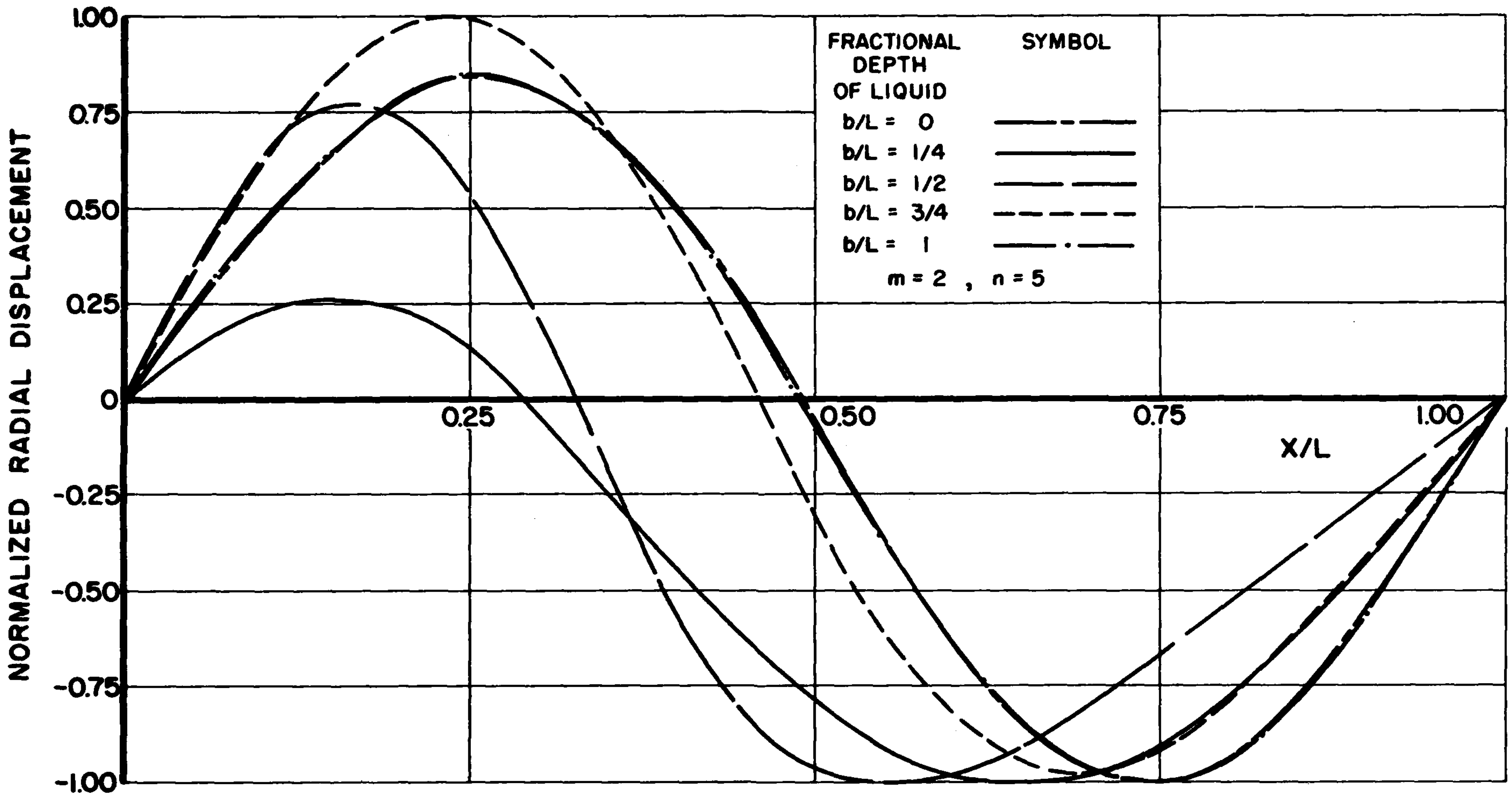

FIGURE 8 Axial Mode Shapes, m = 2, n = 5, at Varying Liquid Depths

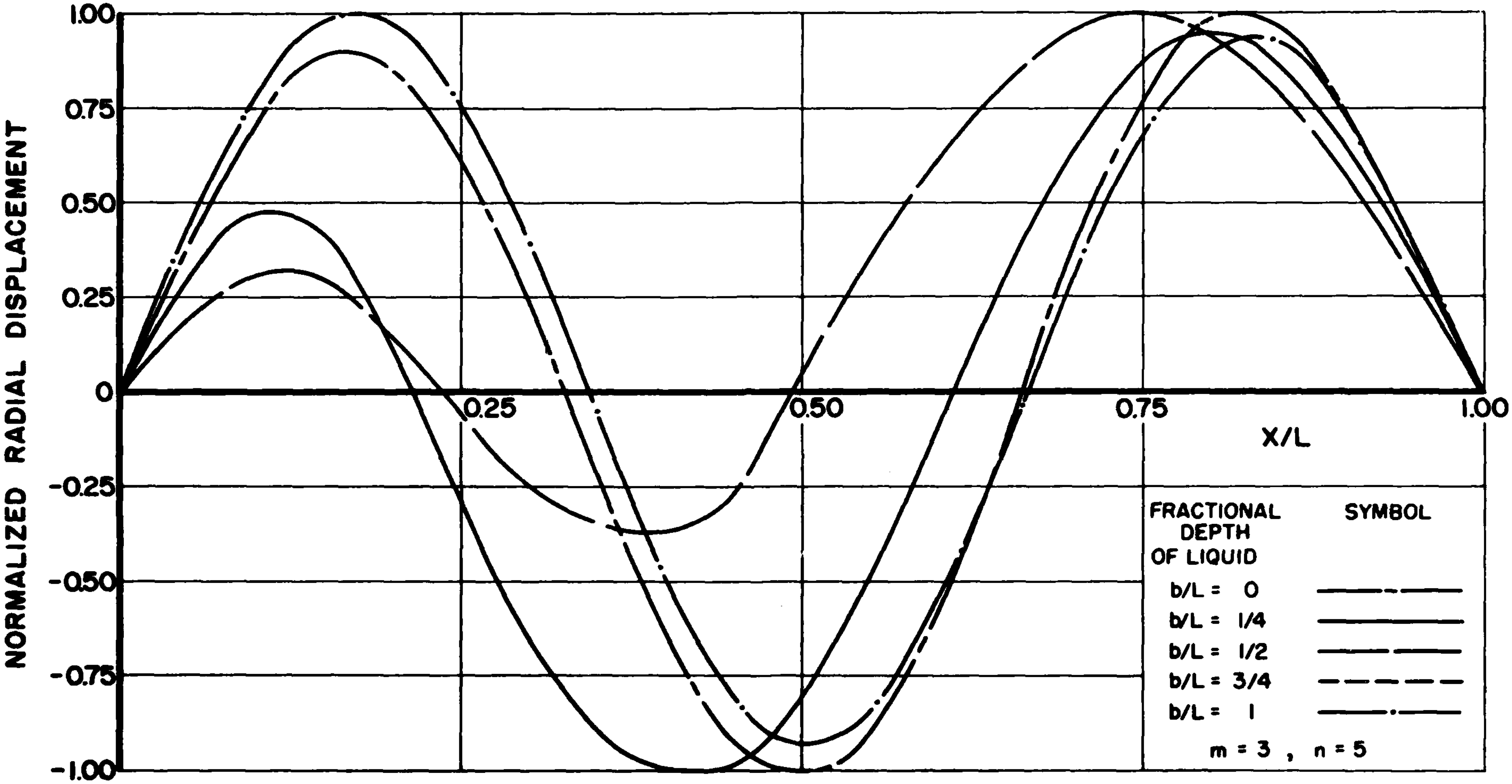

FIGURE 9 Axial Mode Shapes, m = 3, n = 5, at Varying Liquid Depths

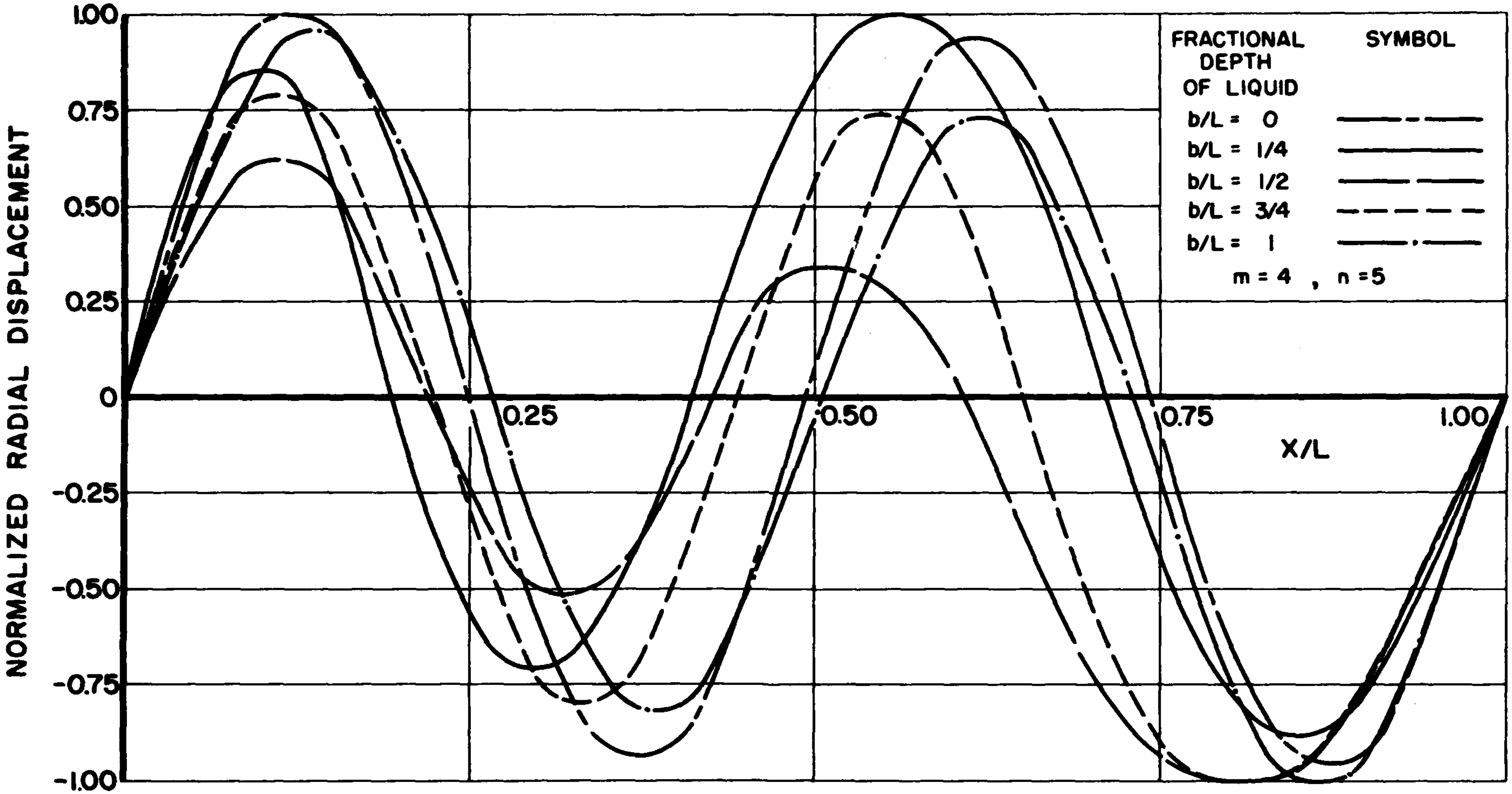

FIGURE 10 Axial Mode Shapes, m = 4, n = 5, at Varying Liquid Depths

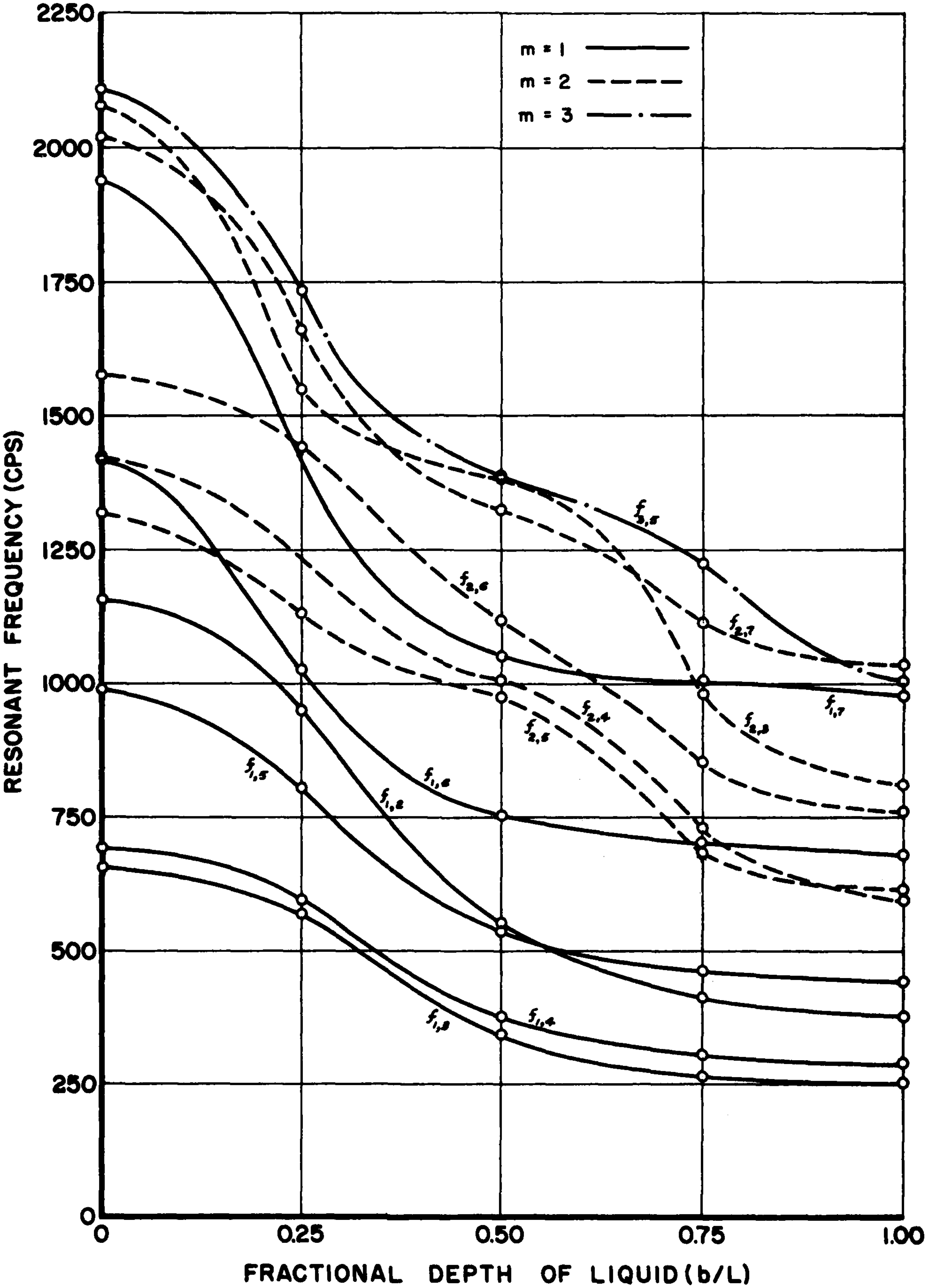

FIGURE 11 Variation of Resonant Frequency With Liquid Depth for Several Breathing Modes

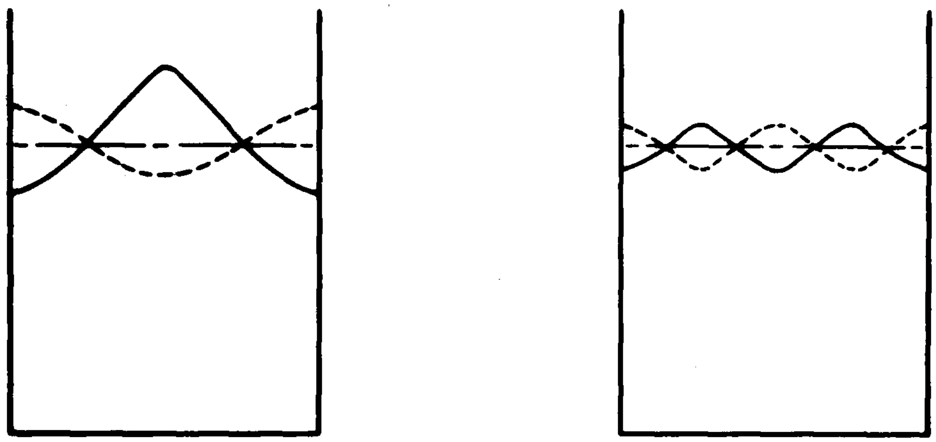

a. FIRST TWO MODES OF LOW FREQUENCY LIQUID RESONANCE

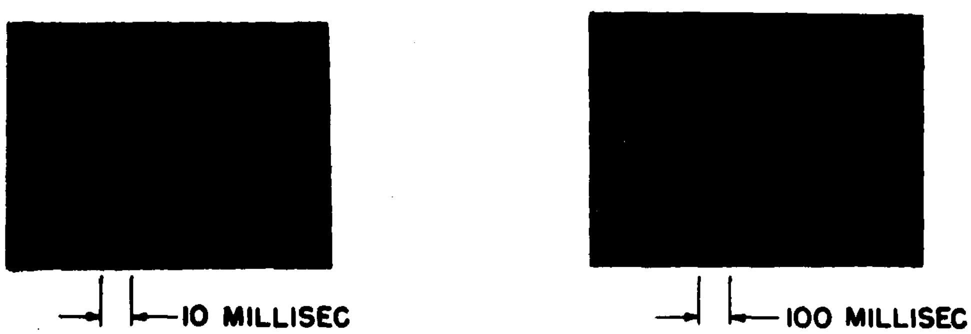

b. OSCILLOSCOPE RECORDS OF WALL DISPLACEMENT DURING LOW FREQUENCY LIQUID RESONANCE

FIGURE 12 First Two Low Frequency Liquid Modes (a) as Excited by the High Frequency (375 cps) Forced Oscillation of the Shell Wall (b). The Beat Frequency in the Wall Displacement Records is 5 cps.